Atmospheric Pollution Research 12 (2021) 101214

Contents lists available at ScienceDirect

Atmospheric Pollution Research

journal homepage: www.elsevier.com/locate/apr

Characterization of unique aerosol pollution episodes in urban areas using TXRF and TXRF-XANES

Ottó Czömpöly [a], Endre Börcsök [a], Veronika Groma [a], Simone Pollastri [b], János Osán [a,*]

[a] Environmental Physics Department, Centre for Energy Research, Konkoly-Thege M. út 29-33, H-1121, Budapest, Hungary
[b] Elettra Sincrotrone Trieste, Strada Statale 14 - km 163, 5, Basovizza, Trieste, I-34149, Italy

ARTICLE INFO

Keywords:
Atmospheric aerosols
TXRF
XANES
Elemental size distribution
Elemental speciation
Cascade impactor

ABSTRACT

Identifying sources of unique, short-time aerosol pollution episodes in urban areas is a difficult task since they could last only for a couple of hours. With the combination of size-fractioned sampling with May-type cascade impactor and total-reflection X-ray fluorescence (TXRF) in addition to X-ray absorption near-edge structure spectroscopy various sources could be identified in samples collected in Budapest (Hungary) and Cassino (Italy). Using short-time (1–4 h), size-fractionated (70 nm up to 10 μm into 7 stages) sampling method, TXRF is capable of detecting transition metals in the order of 0.1 ng/m^3. The present study discusses pollution episodes with Cu and Br concentrations in the range of 1–40 ng/m^3. The contribution of both exhaust and non-exhaust type traffic-related emission sources were found to be dominant in the Cu species. Wear products of brake system were identified in coarse particles in addition to resuspension of roadside dust. The ratio of organic/inorganic Br could be determined for a pollution episode with elevated Br concentration.

1. Introduction

Atmospheric pollution related to fine aerosol particles is becoming more and more investigated topic (Borgese et al., 2020; European Environment Agency, 2020; Pope and Dockery, 2006). Airborne particulate matter (PM) could be originated from both anthropogenic and natural sources. The most important anthropogenic sources are traffic, combustion of fossil fuels and industry-related emissions. The concentration of PM_{10} (PM_x denotes particulate matter with an aerodynamic diameter less than or equal to x μm) exceeds the level recommended by the World Health Organization (WHO) in many densely populated areas (European Environment Agency, 2020). To find tools capable of reducing air pollution efficiently, well-described source profiles are crucial. Identifying pollution sources is a very complex task generally require a lot of input data. Apart from the natural/anthropogenic division of sources, point/diffuse and also unique/regular sources could be partitioned. For apportionment of sources showing a repetitive pattern, statistical models such as positive matrix factorisation (PMF) are usually applied. PMF is a method based on large datasets of concentrations of chemical elements or compounds present in PM (at least one hundred samples) (Clemente et al., 2021; Dai et al., 2021; Jain et al., 2020). PMF model is affected by a bunch of initial conditions and parameters therefore the results rely heavily on pre-adjustments. Regarding PMF, a presumption has to be made regarding the number of factors to retain. Coupling these factors to sources require information of existing source profiles and interpreting these factors can result in equivocal outcomes. Usually, several analytical techniques [like ion chromatography (IC), gravimetry, thermal-optical techniques, inductively coupled plasma optical emission spectrometry (ICP-OES)] are needed to be applied for creating a sufficiently good input matrix which most cases require different sampling techniques. X-ray fluorescence (XRF) analysis can be also used as a tool for the determination of elemental concentrations for building up input matrices for PMF (Perrone et al., 2018).

Identifying unique pollution episodes can be a challenging task since their existence could be only a couple of hours. With appropriate sampling techniques, XRF methods are capable to identify pollution episodes with a time resolution of 1–4 h (Osán et al., 2020), based on elevated elemental concentrations. Since XRF methods are non-destructive, they can be easily combined with other techniques and also leave the possibility for further studies on the very same samples, if needed.

Because of the short time existence and unique characteristics of

Peer review under responsibility of Turkish National Committee for Air Pollution Research and Control.
* Corresponding author.
E-mail address: osan.janos@ek-cer.hu (J. Osán).

https://doi.org/10.1016/j.apr.2021.101214
Received 20 July 2021; Received in revised form 22 September 2021; Accepted 22 September 2021
Available online 25 September 2021

pollution episodes, the sources causing them cannot be derived using the generally applied statistical methods (e.g. PMF), mainly due to the limited number of samples available from the episodes themselves. In order to gain information on the possible sources of pollution episodes, a different approach is proposed, based on the size distribution of elemental concentrations and chemical speciation of elements having elevated atmospheric concentrations during the studied pollution episodes.

When studying environmental samples usually difficult matrixes and multi-phase systems need to be evaluated. Numerous possibilities of origin can come into consideration, even ones which were not taken into account formerly. A good size resolution of aerosol particles has great importance in the process of identifying pollution sources. Individual sources have their own emission characteristics as a function of particle diameter. Crustal erosion and wear products, moreover, sea salt aerosols tend to be present in the coarse particles (1–10 μm) (Angyal et al., 2021; Beuck et al., 2011). These particles can originate directly from sources or by the resuspension of settled particles. Across the fine particles (sub 1 μm region) usually secondary or condensate aerosols and particles emitted during anthropogenic activities can be identified (Habre et al., 2021).

For aerosol pollution sources, chemical speciation of specific elements can also be characteristic, which can be performed non-destructively using X-ray absorption near-edge structure (XANES) spectroscopy, without requiring treatment of the collected PM samples. Sakata et al. (2014) were able to identify a municipal solid waste incinerator as a source of fine aerosol particles containing Pb species combining XANES, ICP-OES, and IC. Although Valotto et al. (2017) studied soil and road-side dust (which can be released to ambient aerosol via resuspension), their work is a great example for the effectiveness of combining different methods. They successfully characterized the collected samples and certified reference materials together with two types of brake pads. The elemental concentrations were determined by ICP-OES after digestion, while the chemical speciation of Cu, Zn, and Sb was studied using XANES. Gunchin et al. (2021) were able to identify the chemical speciation of Cr and Zn on $PM_{2.5}$ and PM_{10} samples applying XANES spectroscopy, where elemental concentrations determined by XRF were the basis of sample selection.

Applications of fluorescence mode XANES using the standard 45°/45° geometry for speciation of elements in aerosol particles collected on filters highlight that a 24–48 h sample collection is necessary for size-resolved studies (Miyamoto et al., 2020; Ouyang et al., 2018; Tirez et al., 2011). In our previous work using total-reflection X-ray fluorescence (TXRF) for determination of size distribution of elemental concentrations in atmospheric aerosols (Osán et al., 2020), pollution episodes lasting only for a few hours could be identified. Thus, XANES spectrometry in TXRF detection geometry can enable a diminishing of the sampling time to a few hours delivering elemental speciation information with high time resolution, allowing study of pollution episodes (Osán et al., 2010).

This study aims to show the capabilities for emission source analysis of unique pollution episodes by the combination of X-ray fluorescence and absorption methods on size-fractionated PM samples. Sampling with May-type cascade impactor and analysis of samples by TXRF were carried out. The selected samples with elevated concentrations of Cu and Br reflecting pollution episodes were studied with synchrotron radiation-based XANES for determining the chemical species being present in each sample. The possible sources were determined based on the elemental size distribution and the chemical species of Cu or Br being present in the samples. As a new approach, besides pure chemicals, PM samples collected near known pollution sources were used as standards for the chemical speciation investigations.

2. Materials and methods

2.1. Samples

2.1.1. Sampling equipment

Aerosol particles were collected using a 9 stage May-type cascade impactor onto 20 × 20 mm^2 polished silicon wafers. Stages 3–9 (cut-off diameter ranges: 9–4.5 μm, 4.5–2.2 μm, 2.2–1.1 μm, 1.1–0.57 μm, 1.1–0.57 μm, 570-290 nm, 290-180 nm, 180-70 nm respectively) were used during the sampling campaign which almost covers the whole PM_{10} region. In the May-type impactor the rectangular-shaped openings consist of a persistent 50 mm long side and a size variant short side, decreasing in the function of stage number. This geometry deposits a thin stripe of particles (0.1 mm–1 mm) on the centre line of the silicon wafers. 4 h of sampling time was found to be optimal with a flow rate of 16.7 l/min (4 m^3 of air is analysed in one sample set). Sampling onto silicon wafers enables to perform multiple analytical techniques on the very same sample (TXRF, XANES, Raman spectroscopy, Scanning electron microscopy, etc.)

2.2. Sampling sites

2.2.1. Cassino

The airborne particle pollution in Cassino, Italy (41°29′16″N, 13°49′32″E) is mostly affected by local traffic sources, as well as natural sources like sea spray. The location of sampling was situated in an urban area of Cassino in the vicinity of a two-ways single-lane road with a traffic density of 24 ± 3 vehicles per minute. The impactor was placed in a second floor window inside the campus of University of Cassino and Southern Lazio. A monitoring station 400 m far from measurement site is operated by the Environmental Protection Agency. The sampling was carried out in September 2018. During the entire sampling campaign significant amount of precipitation was not detected. A cold front in 25 Sept moving over the region split the weather conditions of the campaign into two parts. Between 21 and 24 Sept the average temperature was 24.9 °C with a relative humidity of 72.2%. After the frontal passage lower temperature and relative humidity was recorded, 19.5 °C and 47.1%, respectively. Due to the change in meteorological conditions a drop in the PM_{10} concentration was detected from 22.4 μg/m^3 to 12.3 μg/m^3.

2.2.2. Budapest

Air quality of Budapest, capital city of Hungary, is primarily effected by the great volume of traffic, especially in downtown areas. To control the level of air pollution many monitoring stations are operated which of 12 observes hourly PM_{10} and $PM_{2.5}$ concentrations.

Two urban measurement sites in downtown Budapest were selected, as well as two purposeful sampling site was defined which are linked directly to a local emission source. Sampling site is located in a green belt area in the Buda side of Budapest (47°28′46″N, 19°02′37″E). The measurement site is a first floor balcony 15 m far from a one-way low traffic (1500 cars/day) road, whilst a heavy traffic, double-lane road is situated 300 m far with approximately 7000 cars/day. A Hungarian Air Quality Network station operates within 300 m also. The campaign was performed between 31 July and 9 August in 2019. During this period unstable air mass determined the weather of the region, with traceable amount of precipitation on 2 and 6 of August. The daily mean temperature was 20–26 °C with a daily maximum of 36–31 °C, the average wind speed was 2.4 m/s. A more detailed description of this sampling campaign can be found in our previous study (Osán et al., 2020).

The second urban measurement site was chosen to be also in downtown Budapest, however in the neighbourhood of a big traffic junction (47°30′30″N, 19°01′25″E). The volume of the traffic is 20 000 cars/day on weekdays. The sampling site was also on a balcony facing to the square on the 5th floor. The sampling was carried out during the heating season (Nov 17, 2011), when the weather was stable due to the

presence of a high pressure system over the region. The temperature was slightly above freezing point (5 °C), the maximum wind speed detected was 3 m/s.

2.2.3. Sampling near pollution sources

Two aerosol samples were collected in the vicinity of emission sources (coal burning and diesel smoke). The particulate emission of coal burning was studied at a household multi-fuel tile stove operated using German black coal briquette, in a suburban family house in winter conditions. The sampling inlet was placed right next to the chimney at 14 m height allowing collection of particulate matter directly from the plume. A reduced sampling time of sampling time of 1 h was sufficient to ensure particulate matter load at each impactor stage suitable for TXRF analysis.

The sample representing diesel smoke emission was collected from a heavy duty diesel engine exhaust under indoor laboratory conditions. A RÁBA D10 UTSLL 160 engine typical for the Hungarian bus fleet was operated at 50% load at 1600 rpm. The raw exhaust was directed into a full flow constant volume sampling system including a dilution tunnel, then the exhaust concentration was further reduced by an ejector diluter, resulting in a 100-fold dilution. Even from the diluted diesel engine exhaust, a 5-min sampling time was proved to be sufficient for a successful TXRF evaluation. Particular circumstances of the sampling and the studied parameters are detailed in the work of Ajtai et al. (2016).

2.3. Analytical methods

2.3.1. TXRF

For the present study a compact low-power TXRF configuration was applied. A 50 W Mo-anode X-ray tube with a multilayer monochromator is used which selects Mo-Kα X-ray as excitation source. The X-ray tube was always operated at maximum power, 50 kV and 1 mA. For recording X-ray spectra, a 7 mm^2 silicon drift detector (SDD) with Zr collimator ring (AXAS-A, Ketek, Germany) was applied. The processing of the signal was carried out by an analogue signal processing unit (System 8000, PGT, USA). Considering counting time, measurements typically took 3000 s long and were performed in air. The X-ray spectra were processed with QXAS AXIL and PyMCA software packages (Solé et al., 2007; Vekemans et al., 1994).

Determination of the concentration of elements in the aerosol samples was based on external standard, prepared using a multielemental ICP standard solution (Merck IV). Via a nanoliter injector (WPI, USA) droplets (1 ng/droplet) were deposited with 1-mm spacing on the centreline of the 20 × 20 mm^2 silicon wafers. With this arrangement the standards were measured in the same geometry (±100 μm precision) as in case of the collected environmental samples. The deposited line was placed horizontally during the TXRF analysis, perpendicular to the collimated (10 mm × 100 μm) exciting beam. These standards were essential for determining sensitivities relative to chromium. Absolute mass was determined using standard samples containing chromium pads deposited onto silicon wafers using microlithography. The deposited Cr pads contain 4 ng or 8 ng chromium (±5%) within a 50 nm and 100 nm height, respectively. The Cr pads are situated around the centreline in a 350 μm wide band. The homogeneity of the deposited line on the silicon wafer was tested previously via synchrotron based TXRF showing a deviation within 3% (Groma et al., 2008). The atmospheric concentrations are calculated from the mass determined by TXRF as a function of the collected air volume.

Due to the high sensitivity of the TXRF system, detection limits in the 10 pg range (per sample) can be reached for transition metals and Pb, allowing for a short sampling time of 1–4 h (Osán et al., 2020). By applying a detector with larger active area (50 mm^2 instead of 7 mm^2), even the measurement time could be reduced by an order of magnitude resulting in an increased analytical throughput of the method (Bilo et al., 2018; Borgese et al., 2020; Prost et al., 2017).

Summarizing all stages analytic results for each sampling the elemental size distribution can be determined, which gives the relative abundance for each studied element as a function of aerodynamic particle diameter (d_p).

2.3.2. X-ray absorption near edge structure spectroscopy (XANES)

The XANES measurements were carried out at the XRF beamline of Elettra Sincrotrone Trieste (Basovizza, Italy). XANES spectra at Cu and Br K-edges for the selected samples were collected using a Si (111) monochromator, in fluorescence mode using an XFlash 5030 SDD (Bruker, Berlin, Germany). Energy calibration of the monochromator was achieved prior the measurement of samples using Pt foil (L_3-edge) for Br and Cu foil for Cu. The energy step size varied between 0.5 and 5 eV in the pre- and post-edge region, meanwhile it was 0.2 eV in the near-edge region. The deposited line was oriented parallelly with the collimated (100 × 200 μm) incident beam. The silicon wafers were aligned in total-reflection geometry to achieve the lowest detection limit possible. Full TXRF spectra were collected at each energy position, and fluorescence mode XANES spectra were recorded based on the Kα peak intensities of the element of interest (I_f) and the incident beam intensity measured by a diamond beam monitor (I_0) while tuning the excitation energy with the Si(111) monochromator (Karydas et al., 2018). With the purpose to reach XANES spectra of good statistics, several scans were recorded merged and then normalized. The chemical states of selected elements were determined using linear combination fitting (LCF) of standard spectra with Athena module of the IFEFFIT package (Ravel and Newville, 2005). The fitting parameters were set to apply maximum 4 standards and the LCF was performed in the range of −20 eV and +60 eV relative to the absorption edge. Reference spectra were acquired from pure compounds (Cu, Cu_2O, CuCl, $Cu_3(CO_3)_2(OH)_2$, CuBr, CuO, $CuCl_2$, $CuBr_2$, CuS) in the form of pressed pellets, containing 2% of the element of interest mixed with polyvinylpyrrolidone binder (Fig. 1).

3. Results and discussion

This study involves the analysis of samples collected directly from sources and also from urban environment. The two aerosol samples collected in exhaust plumes (coal burning and diesel smoke) were involved into LCF evaluation of environmental samples. First, XANES spectra of these two source-specific samples were fitted with spectra of pure compounds, then beside pure compounds spectra, these results were considered as standards for the environmental samples in the LCF to determine their possible contribution. The selection of urban PM samples for XANES measurements was based on the results of TXRF analysis. Primarily Cu and Br concentrations were taken into consideration (Table 1). The Cu and Br XANES results are discussed together with the normalized elemental size distributions, which are presented as $\Delta C/\Delta \log d_p/C$ (Fig. 2). As the argument of log function needs to be dimensionless, d_p stands for relative particle diameter (−) and C is the total concentration of the measured size fractions (70 nm–9 μm) determined by TXRF in ng/m^3. This way the areas under the curves are equal to one. The calculated values are plotted in the function of the representative diameter (which is the geometric mean of the cut-off diameters for each stage in our case). The reason for presenting the size distributions normalized to the total concentration is that both major and minor components can be plotted on the same figure despite that two or even three order of magnitude difference can occur in their concentrations. By presenting all elements on the same figure the differences and similarities in the shape of size distributions are clearly noticeable. Elements having size distribution of similar shape can be assumed to be linked to the same emission sources. The determined total elemental concentrations are indicated in the figures (Fig. 2) next to the legend of each element in ng/m^3. Out of 51 sample sets, 5 interesting episode was selected (Table 1). In case of Episode A, 5 stages from the diameter range of 180 nm to 4.6 μm were measured and evaluated with Cu–K XANES. LCF results (Table 3) reveal a trend which is in accordance with the pre-hypothesis, which states that the wear products containing Cu are most

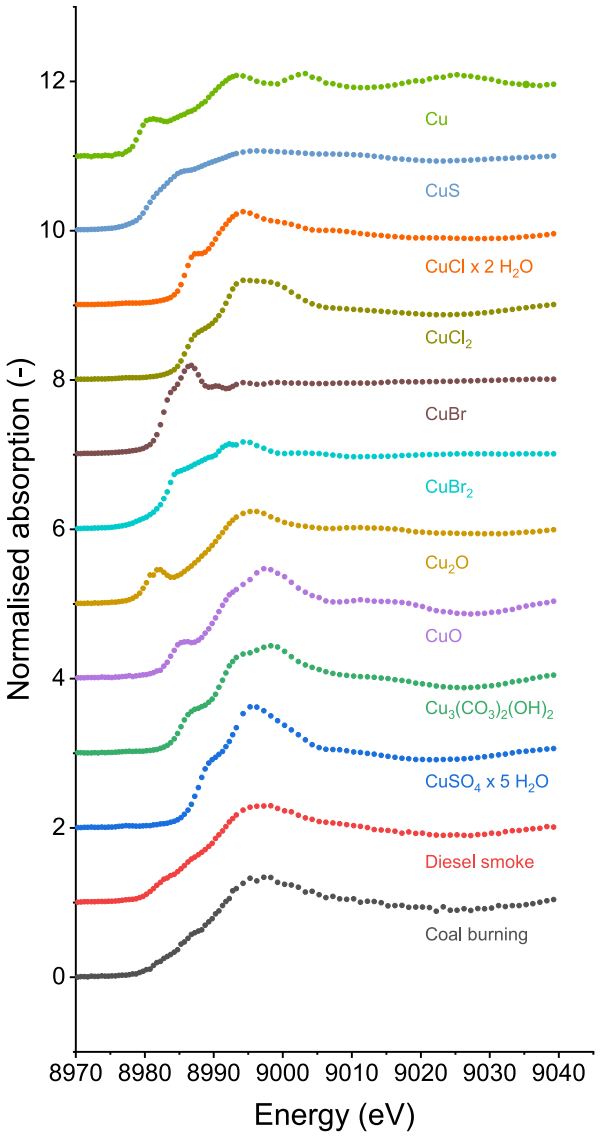

Fig. 1. Cu K-edge XANES spectra of standards of pure compounds and samples collected at sources (coal burning and diesel smoke).

Table 1
Features of the selected pollution episodes.

Episode	Location	Date	Time	Characteristics	Markers
A	Budapest, Széna tér	Nov 17, 2011	20:00–21:00	High traffic location	Coarse: Cu, Fe, Ca Fine: S, K, Zn
B	Cassino	27 Sept 2018	10:45–15:50	Sea salt	Coarse: Cl
C	Budapest, Ménesi út	Aug 2, 2019	06:00–10:00	Resuspension	Coarse: K, Ca, Fe
D	Budapest, Ménesi út	Aug 2, 2019	16:00–20:00	Resuspension	Coarse: K, Ca, Fe
E	Budapest, Ménesi út	Aug 6, 2019	06:00–10:00	High Br episode	Fine: Br (Cu, S, K)

dominant in the coarse fraction, while the species connected to exhaust products are abundant in the fine fraction. After making sure it meets the preliminary expectations, the stage with highest concentration of Cu was measured with XANES for all selected episodes (Fig. 3). Episode E is special in the way that not only one Cu but also Br concentration is high, therefore XANES spectra for Br were collected as well .

3.1. Samples from direct sources

3.1.1. Coal burning

This sample was collected from the exhaust resulting from black coal burning, thus a wide range of elements was identified. Cu shows similar elemental size distribution as Br, Cl and S. K is most abundant in finer particles and its peak maximum is around 0.2–0.3 μm (Fig. 2f). In comparison, Saarnio et al. (2014) studied the particle emission of a coal-powered power plant and studied size distribution of main and trace components. Their chemical mass size distribution shows a bimodal characteristic, with a smaller peak between 0.1 and 0.2 μm and a more significant one around 0.5–0.6 μm. Regarding the Cu–K XANES results, Cu is mostly in the form of $Cu_3(CO_3)_2(OH)_2$ and in forms containing S (CuS, $CuSO_4$) (Table 2). In the linear combination, Cu, $CuCl \cdot 2H_2O$, Cu_2O, CuBr, $CuCl_2$ and $CuBr_2$ standard spectra were also applied, but in the first 9 combinations out of 10 with lowest χ_r^2 these standards were not involved.

3.1.2. Diesel smok e

Direct sampling from diluted diesel engine exhaust resulted that concentration of Zn significantly high, due to the presence of lubricating oil present in the combustion area. Zn dialkyldithiophosphates are commonly added to lubricating oils as they have a corrosion and oxidation inhibitor characteristic (Ratoi et al., 2014). Cu can originate from various parts of diesel engine, from both combustion and wear-related sources (La Rocca et al., 2020). Lubricant oil can interact with the cooler core resulting in release of Cu species. Cu is a metallurgical component of brass and bronze, which is found in bushings and bearings inside an engine. Half of the copper species present in this sample was identified as S containing ones (CuS, $CuSO_4$), however $Cu_3(CO_3)_2(OH)_2$ is present in lower concentration than in coal burning. CuO has the same ratio in both studied sources (Table 2).

3.2. Samples collected during pollution episodes

3.2.1. Episode A

Cu, Fe and Ca were found to be present in elevated concentration in the coarse fraction (Fig. 2a). Cu and Fe are most likely products of abrasion-related processes. Evaluating XANES measurements, CuS showed increasing tendency with particle size. As Valotto et al., 2017 reported, the car brake pads mostly consist of CuS, the presence of break wear products in this episode is assumable. LCF fitted low ratio of diesel smoke in coarse mode, but around 2 μm the contribution of this source appears. The relevance of diesel smoke is highest around 0.3 μm which is in accordance with the characteristics of diesel engine emission. Since this sample set was collected at a very populated and busy location of Budapest, a great contribution of traffic to the pollution episode could be identified. Ca is a marker of erosion and resuspension activities. S shows a peak maximum located around 0.5 μm (Fig. 2a), which is related to anthropogenic activities. Results shows an enormous decrease in the amount of S in the coarse fraction. This kind of distribution is a sign of secondary formation and ageing of SO_4 species from sulphur oxides gases.

3.2.2. Episode B

Across the Cassino series, three types of distribution are present (Fig. 2b). K, S and Br are abundant in the accumulation mode peaking at 0.25 μm, while the coarse mode is dominated by Fe, Cu, Ca and Cl, but the size distribution of Cl shows a sharper peak at around 9 μm. The observed rising concentration in the coarse fraction can be described by the sea-salt origin of Cl, as this sample was collected in Cassino located near the sea. In the coarse fraction, LCF revealed the presence of elemental copper as well as CuS (31 ± 2%). Cu (17 ± 2%) in the coarse

Table 2
LCF results of samples representing sources. The goodness of fit is represented by the *R*-factor and the reduced χ square (χ_r^2).

	CuO	$Cu_3(CO_3)_2(OH)_2$	CuS	$CuSO_4{\cdot}5H_2O$	*R*	χ_r^2
Coal Burning	15 ± 5	41 ± 5	26 ± 1	16 ± 3	1.76E-03	3.70E-04
Diesel Smoke	15 ± 3	32 ± 4	35 ± 1	17 ± 2	1.46E-03	2.61E-02

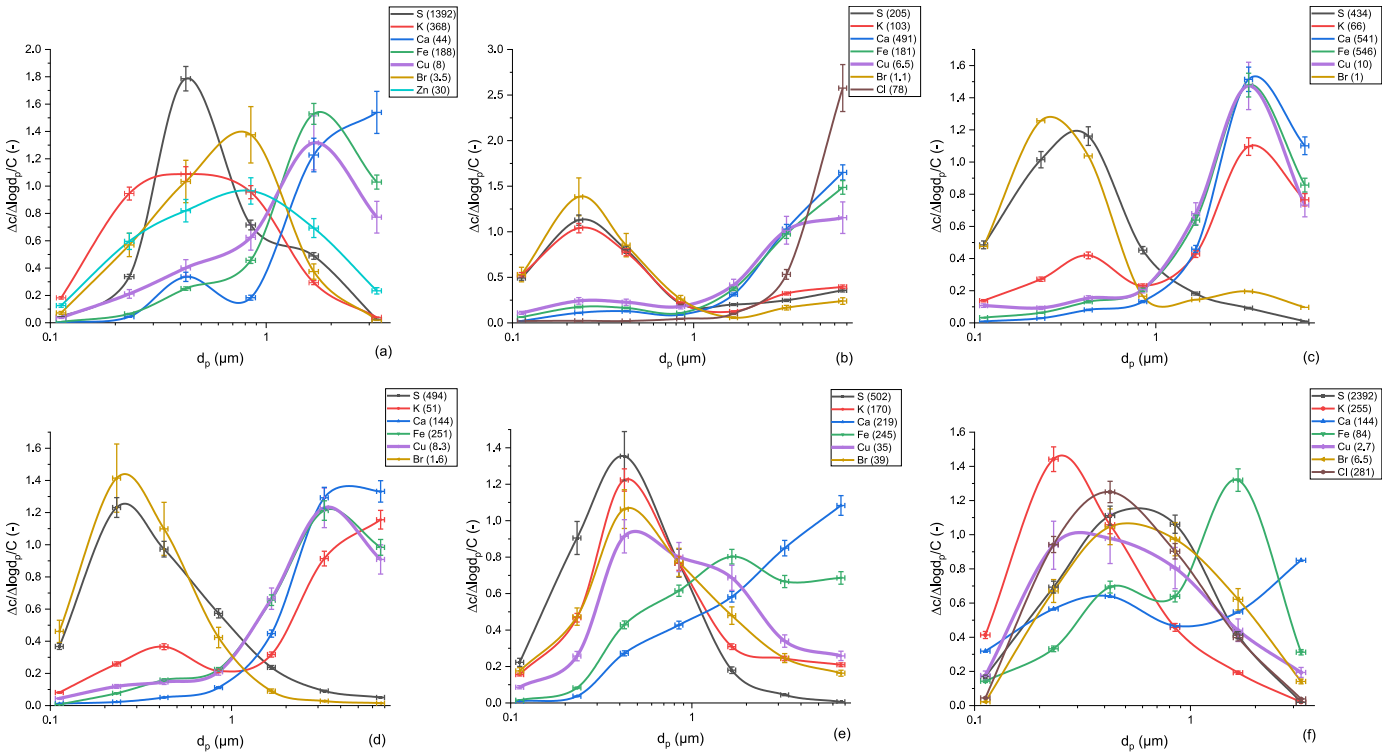

Fig. 2. Normalized elemental size distribution of particles collected during Episode A (a), Episode B (b), Episode C (c), Episode D (d), Episode E (e) and of particles originated from coal burning (f). The determined total elemental concentrations in ng/m^3 are presented next to each element in brackets. Error bars represent 1σ (standard deviation).

Table 3
Relative abundances (%) of Cu species derived from LCF results in selected aerosol size fractions of the five pollution episodes. The goodness of fit is represented by the *R*-factor and the reduced χ square (χ_r^2).

	Coal burning	Diesel Smoke	Cu	$CuCl{\cdot}2H_2O$	Cu_2O	CuBr	$CuCl_2$	$CuBr_2$	CuO	$Cu(CO_3)_2(OH)_2$	CuS	$CuSO_4{\cdot}5H_2O$	*R*	χ_r^2
Episode A 2.4–4.8 μm		6 ± 6			27 ± 3						66 ± 3	3 ± 3	1.87E-03	2.60E-04
Episode A 1.2–2.4 μm		54 ± 6									33 ± 3	18 ± 3	1.19E-03	2.15E-04
Episode A 0.6–1.2 μm		74 ± 5			5 ± 2		12 ± 3				10 ± 2		1.18E-03	2.10E-04
Episode A 0.3–0.6 μm		81 ± 6					11 ± 4				8 ± 2		1.71E-03	3.10E-04
Episode A 0.18–0.3 μm	19 ± 7	82 ± 6											1.09E-03	2.02E-04
Episode B 2.4–4.8 μm			17 ± 2				18 ± 3		31 ± 3		31 ± 2		2.5E-03	4.95E-04
Episode B 0.18–0.3 μm		58 ± 4		7 ± 3					20 ± 4			10 ± 2	2.53E-03	5.92E-04
Episode C 2.4–4.8 μm			8 ± 2							22 ± 2	57 ± 2	13 ± 2	1.79E-03	1.70E-02
Episode D 2.4–4.8 μm										28 ± 3	51 ± 3	18 ± 3	3.89E-03	6.67E-04
Episode E 0.3–0.6 μm					28 ± 3			22 ± 2		18 ± 3		27 ± 2	4.00E-03	6.30E-04

fraction with elevated concentration is a marker of abrasion type traffic related pollution. Motorbike brakepads are almost entirely built-up of elemental copper, but Valotto et al. (2017) reported the presence of CuS and Cu(0) also in car brake pads in their study. Across the fine particles, $CuSO_4$ (10 ± 2%) was identified, whilst there is an absence of CuS. The contribution of diesel smoke was found to be dominant (58 ± 4%) in the

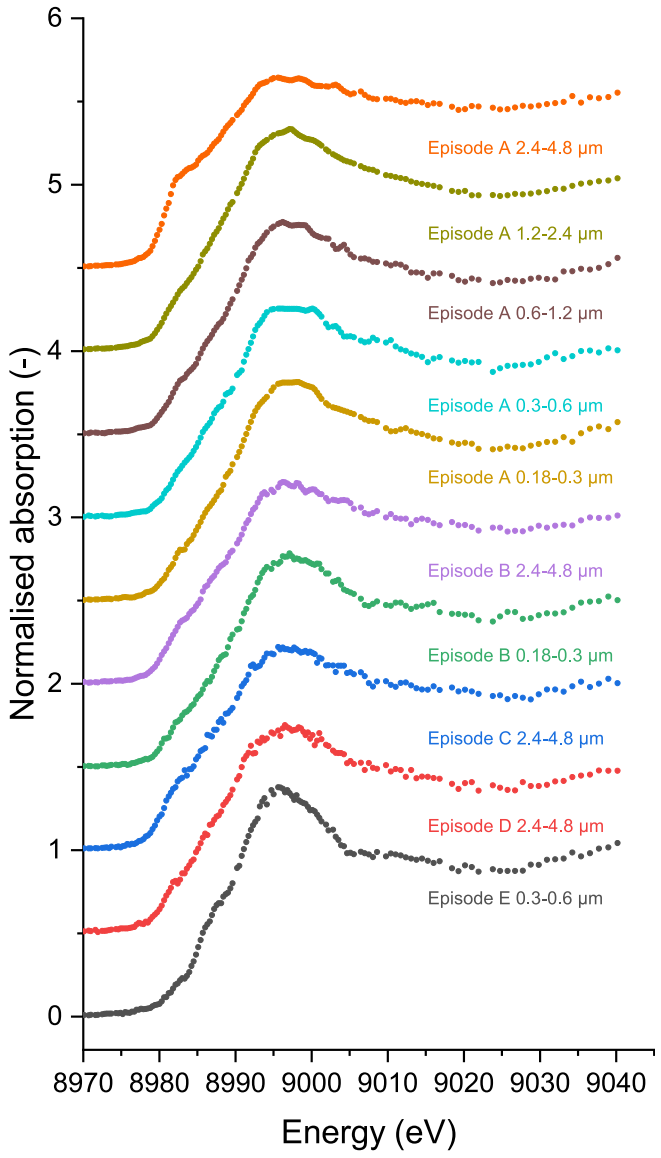

Fig. 3. Cu–K edge XANES spectra of selected size fractions of urban aerosol samples collected during the five pollution episodes.

fine fraction (180–290 nm). Significant amount of S and K were identified across the fine particles, meanwhile in the coarse fraction their concentration drops by a factor of three. The high S and K concentration in the fine fraction could be the result of secondary aerosol formation, condensation and accumulation (mainly connected to anthropogenic activities). K present in the coarse fraction is the result of erosion and soil resuspension. The role of traffic was found to be responsible for at least one half of collected Cu during this pollution episode, which conclusion is based on the ratio of the wear products of brake systems in the coarse fraction and on the dominance of diesel smoke across the fine fraction particles.

3.2.3. Episode C

The elemental size distribution of Ca, Fe, and Cu shows the highest concentration in the coarse particles, which suggests the presence of erosion and wearing-related pollution sources (Fig. 2c). XANES LCF analyses of Stage 4 (d_p = 2.2–4.5 µm) indicates the presence of metallic Cu (8 ± 2%) and also a great amount of CuS (57 ± 2%). $Cu_3(CO_3)_2(OH)_2$ appears in the combinatorial results, so a natural contribution to the pollution episode is assumable also (see Fig. S1 in Supporting Information). K has a bimodal size distribution, thus the contribution of resuspended soil can be clearly identified as well as the effect of anthropogenic activities as a secondary peak shows up, mainly in condensation mode. S has an unimodal distribution with a maxima in the condensation mode (around 0.3 µm). Regarding the sources of Cu, resuspension of road-side dust containing wear products of brake system could be apportioned. Particles originated from crustal erosion are also present since Ca have elevated concentration in the coarse mode, so a natural contribution to this pollution episode is assumed.

3.2.4. Episode D

Episode D is very similar to Episode C from the aspect of elemental size distribution, however lower contribution of traffic was found. as the LCF results show smaller contribution of brake wear to the concentration of Cu. Also the metallic Cu in this case was not identified and the ratio of CuS has changed from 57 ± 2% to 51 ± 3%. The ratio of $Cu_3(CO_3)_2(OH)_2$ and $CuSO_4$ elevated from 22 ± 2% to 28 ± 3% and from 13 ± 2% to 18 ± 3%, respectively. The concentration of Ca is lower by a factor of 3 and the concentration of Fe drops to half compared to Episode C. The normalized abundance of elements (Fig. 2d) in the coarse mode is lower by 10% than it was in the previous episode. While the resuspension of road-side dust was the main source during Episode C, in case of this episode beside resuspension heavy anthropogenic particle emission is present.

3.2.5. Episode E

During this episode twenty times higher Br concentration was observed than average concentration measured during the sampling campaign. The concentration of Br returned to normal after a few hours as published in our previous work (Osán et al., 2020). Br, S, K and Cu elemental size distribution show similarities with the peak maximum around 0.6 µm (Fig. 2e). Because of the similarities in the size distribution same emission source can be linked to all three elements. Cu–K LCF results of Stage 7 (d_p = 570-290 nm) (see Fig. S2 in Supporting Information) show a significant presence 29 ± 3% of Cu_2O (copper(I) oxide), which can be a marker of thermal events involving copper species. In accordance with the TXRF measurements, 21 ± 2% of $CuBr_2$ was fitted during evaluation. Among LCF fittings 6 of 7 fits with lowest reduced χ square contained copper-bromide. Also, elevated amount of $CuSO_4$ (28 ± 2%) was fitted in this sample, which is almost two times

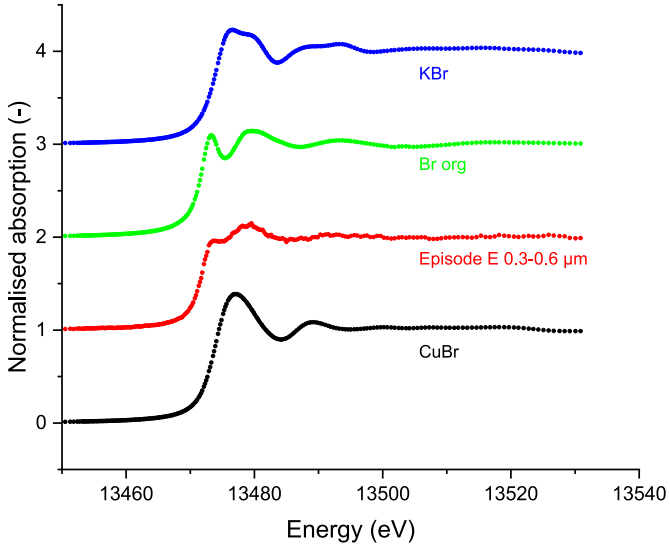

Fig. 4. Br–K XANES spectrum of the measured sample (Episode E) and the standard spectra employed for LCF. The spectrum named "Br org" (1,4-Dibromobenzene) was used to represent the characteristic shape of organic Br compounds.

higher than the average of other samples collected at this location of Budapest. Br–K measurements were also performed on this sample (Fig. 4). Despite that only limited amount of Br reference spectra were available, the ratio of organic and inorganic Br being present could be determined. Since organic bromine compounds have a very characteristic post-edge peak, its abundance have a good reliability (69 ± 5%, see Table 4). The inorganic species were approximated with the spectra of CuBr and KBr. The organic bromine was represented with the reference spectra of 1,4-Dibromobenzene applied from the XANES standard database of Hephaestus (Ravel and Newville, 2005). LCF of the Br–K XANES spectrum is presented in Fig. S3 (Supporting Information). Compounds containing bromine have several anthropogenic utilisations like flame retardants, pesticides/biocides, dyes etc. (Vainikka and Hupa, 2012). Most probably a unique, local source resulted in this pollution episode. The elevated concentration of $CuSO_4$ and Br suggests that the source of this episode could be spraying, but waste combustion cannot be excluded from the possibilities.

4. Conclusions

TXRF analysis in combination with May-type impactor sampling was found to be a useful tool for obtaining elemental size distributions and identifying unique pollution episodes with an optimal time resolution (4 h) with a detection limit of 0.1 ng/m^3 for transition metals. As quantification is based on external standards the post-processing of raw spectra is fast and easy. The high elemental sensitivity of a compact laboratory or a portable TXRF instrumentation with large sensitive area X-ray detector will allow much shorter measuring times increasing the analytical throughput of the method. Elemental size distribution provides useful information on the origin of pollution episodes, but several possibilities can come into consideration during source apportionment evaluation. Revealing the chemical species being present in each sample can reduce the number of potential sources of emission. Samples collected on Si wafers has the advantage to perform further XANES measurements whereby the speciation of the elements of interest can be studied. Fluorescence mode XANES investigations in the total-reflection geometry could be performed on the very same samples on which laboratory TXRF measurements were done. Because of the low mass of the elements of interest on the samples, synchrotron radiation was required as a tunable excitation source with high energy resolution to record the energy-dependent fluorescence signal around the absorption edges. Recent source apportionment studies of aerosol pollution are mostly carried out by PMF dealing with large datasets. In contrary, TXRF method combined with cascade impactor sampling can identify unique pollution episodes from short-term field campaigns. Sources of particulate matter on selected samples with elevated concentrations of Cu and Br were identified based on their elemental size distribution and chemical speciation. In the coarse fraction elemental Cu can be linked to the wear of motorcycle brake pads, while CuS is originated from the abrasion of braking system of automobiles. Elevated concentration of Cu in the accumulation mode at high-traffic locations is caused by the emission of diesel engines. If several elements show a similar and characteristic shape of size distribution, then supposedly their emission sources are the same. The presence of Cu, Br, and S at high concentration in the accumulation mode with peak maxima close to each other in the size distributions is caused by anthropogenic activities. Spraying of pesticides can increase the amount of $CuSO_4$ among the Cu species, and flame retardants can cause elevated concentration of halogenides in the aerosol particles. Collecting and analysing more and more source representing aerosol samples will contribute to a widely applicable source apportionment of unique pollution episodes.

Declaration of competing interest

The authors declare that they have no known competing financial interests or personal relationships that could have appeared to influence the work reported in this paper.

Table 4
Br–K LCF results of Episode E. The goodness of fit is represented by the *R*-factor and the reduced χ square (χ_r^2).

	Br organic	KBr	CuBr	*R*	χ_r^2
Episode E 0.3–0.6 μm	69 ± 1	13 ± 3	16 ± 3	9.66E-04	2.00E-04

Acknowledgements

This work was supported by the European Structural and Investment Funds jointly financed by the European Commission and the Hungarian Government under grant no. VEKOP-2.3.2-16-2016-00011 and the EMPIR programme co-financed by the Participating States and from the European Union's Horizon 2020 research and innovation programme, through grant agreement 19ENV08 AEROMET II. The research leading to this result has also been supported by the project CALIPSOplus under Grant Agreement 730872 from the EU Framework Programme for Research and Innovation HORIZON 2020 (Elettra Nr. 20185437 and 20190593). We also acknowledge the staff of XAFS and XRF beamlines of Elettra Sincrotrone Trieste for collecting the data during in-house beamtime.

Appendix A. Supplementary data

Supplementary data to this article can be found online at https://doi.org/10.1016/j.apr.2021.101214.

Credit author statement

Ottó Czömpöly: Conceptualization, Methodology, Investigation, Writing – original draft, Endre Börcsök: Investigation, Writing – review & editing, Veronika Groma: Investigation, Data curation, Writing – review & editing; Simone Pollastri: Investigation, Writing – review & editing, János Osán: Conceptualization, Methodology, Investigation, Writing – review & editing, Funding acquisition.

References

Ajtai, T., Pintér, M., Utry, N., Kiss-Albert, G., Gulyás, G., Pusztai, P., Puskás, R., Bereczky, Szabados, G., Szabó, G., Kónya, Z., Bozóki, Z., 2016. Characterisation of diesel particulate emission from engines using commercial diesel and biofuels. Atmos. Environ. 134, 109–120. https://doi.org/10.1016/j.atmosenv.2016.03.046.

Angyal, A., Ferenczi, Z., Manousakas, M., Furu, E., Szoboszlai, Z., Török, Z., Papp, E., Szikszai, Z., Kertész, Z., 2021. Source identification of fine and coarse aerosol during smog episodes in Debrecen, Hungary. Air Quality, Atmosphere & Health 1–16. https://doi.org/10.1007/s11869-021-01008-8.

Beuck, H., Quass, U., Klemm, O., Kuhlbusch, T.A.J., 2011. Assessment of sea salt and mineral dust contributions to PM10 in NW Germany using tracer models and positive matrix factorization. Atmos. Environ. 45 (32), 5813–5821. https://doi.org/10.1016/j.atmosenv.2011.07.010.

Bilo, F., Borgese, L., Wambui, A., Assi, A., Zacco, A., Federici, S., Eichert, D.M., Tsuji, K., Lucchini, R.G., Placidi, D., Bontempi, E., Depero, L.E., 2018. Comparison of multiple X-ray fluorescence techniques for elemental analysis of particulate matter collected on air filters. J. Aerosol Sci. 122, 1–10. https://doi.org/10.1016/J.JAEROSCI.2018.05.003.

Borgese, L., Bilo, F., Zacco, A., Federici, S., Mutahi, A.W., Bontempi, E., Trzepla, K., Hyslop, N., Yatkin, S., Wobrauschek, P., Prost, J., Ingerle, D., Depero, L.E., 2020. The assessment of a method for measurements and lead quantification in air particulate matter using total reflection X-ray fluorescence spectrometers. Spectrochimica Acta - Part B Atomic Spectroscopy 167, 105840. https://doi.org/10.1016/j.sab.2020.105840.

Clemente, Yubero, E., Galindo, N., Crespo, J., Nicolás, J.F., Santacatalina, M., Carratala, A., 2021. Quantification of the impact of port activities on PM10 levels at the port-city boundary of a mediterranean city. J. Environ. Manag. 281, 111842. https://doi.org/10.1016/j.jenvman.2020.111842.

Dai, Q., Ding, J., Song, C., Liu, B., Bi, X., Wu, J., Zhang, Y., Feng, Y., Hopke, P.K., 2021. Changes in source contributions to particle number concentrations after the COVID-19 outbreak: insights from a dispersion normalized PMF. Sci. Total Environ. 759, 143548. https://doi.org/10.1016/j.scitotenv.2020.143548.

European Environment Agency, 2020. Air Quality in Europe - 2020 Report. https://www.eea.europa.eu//publications/air-quality-in-europe-2020-report.

Groma, V., Osán, J., Török, S., Meirer, F., Streli, C., Wobrauschek, P., Falkenberg, G., 2008. Trace element analysis of airport related aerosols using SR-TXRF. Idojaras 112 (No.2), 83–97.

Gunchin, G., Osan, J., Migliori, A., Shagjjamba, D., Streli, C., 2021. Chromium and zinc speciation in airborne particulate matter collected in ulaanbaatar, Mongolia, by X-ray absorption near-edge structure spectroscopy. Aerosol and Air Quality Research 21. https://doi.org/10.4209/aaqr.210018, 210018–210018.

Habre, R., Girguis, M., Urman, R., Fruin, S., Lurmann, F., Shafer, M., Gorski, P., Franklin, M., McConnell, R., Avol, E., Gilliland, F., 2021. Contribution of tailpipe and non-tailpipe traffic sources to quasi-ultrafine, fine and coarse particulate matter in southern California. J. Air Waste Manag. Assoc. 71 (2), 209–230. https://doi.org/10.1080/10962247.2020.1826366.

Jain, S., Sharma, S.K., Vijayan, N., Mandal, T.K., 2020. Seasonal characteristics of aerosols (PM2.5 and PM10) and their source apportionment using PMF: a four year study over Delhi, India. Environ. Pollut. 262, 114337. https://doi.org/10.1016/j.envpol.2020.114337.

Karydas, A.G., Czyzycki, M., Leani, J.J., Migliori, A., Osan, J., Bogovac, M., Wrobel, P., Vakula, N., Padilla-Alvarez, R., Menk, R.H., Gol, M.G., Antonelli, M., Tiwari, M.K., Caliri, C., Vogel-Mikuš, K., Darby, I., Kaiser, R.B., 2018. An IAEA multi-technique X-ray spectrometry endstation at Elettra Sincrotrone Trieste: benchmarking results and interdisciplinary applications. J. Synchrotron Radiat. 25 (1), 189–203. https://doi.org/10.1107/S1600577517016332.

La Rocca, A., Ferrante, A., Haffner-Staton, E., Cairns, A., Weilhard, A., Sans, V., Carlucci, A.P., Laforgia, D., 2020. Investigating the impact of copper leaching on combustion characteristics and particulate emissions in HPCR diesel engines. Fuel 263, 116719. https://doi.org/10.1016/j.fuel.2019.116719.

Miyamoto, C., Sakata, K., Yamakawa, Y., Takahashi, Y., 2020. Determination of calcium and sulfate species in aerosols associated with the conversion of its species through reaction processes in the atmosphere and its influence on cloud condensation nuclei activation. Atmos. Environ. 223, 117193. https://doi.org/10.1016/j.atmosenv.2019.117193.

Osán, J., Börcsök, E., Czömpöly, O., Dian, C., Groma, V., Stabile, L., Török, S., 2020. Experimental evaluation of the in-the-field capabilities of total-reflection X-ray fluorescence analysis to trace fine and ultrafine aerosol particles in populated areas. Spectrochimica Acta - Part B Atomic Spectroscopy 167, 105852. https://doi.org/10.1016/j.sab.2020.105852.

Osán, J., Meirer, F., Groma, V., Török, S., Ingerle, D., Streli, C., Pepponi, G., 2010. Speciation of copper and zinc in size-fractionated atmospheric particulate matter using total reflection mode X-ray absorption near-edge structure spectrometry. Spectrochimica Acta - Part B Atomic Spectroscopy 65 (12), 1008–1013. https://doi.org/10.1016/j.sab.2010.11.002.

Ouyang, J., Yang, G.S., Ma, L.L., Luo, M., Zheng, L., Huo, Q., Zhao, Y.D., Hu, T.D., Cai, Z. F., Xu, D.D., 2018. Chlorine levels and species in fine and size resolved atmospheric particles by X-ray absorption near-edge structure spectroscopy analysis in Beijing, China. Chemosphere 196, 393–401. https://doi.org/10.1016/J.CHEMOSPHERE.2017.12.126.

Perrone, M.G., Vratolis, S., Georgieva, E., Török, S., Šega, K., Veleva, B., Osán, J., Bešlić, I., Kertész, Z., Pernigotti, D., Eleftheriadis, K., Belis, C.A., 2018. Sources and geographic origin of particulate matter in urban areas of the Danube macro-region: the cases of Zagreb (Croatia), Budapest (Hungary) and Sofia (Bulgaria). Sci. Total Environ. 619–620, 1515–1529. https://doi.org/10.1016/j.scitotenv.2017.11.092.

Pope, C.A., Dockery, D.W., 2006. Health effects of fine particulate air pollution: lines that connect. J. Air Waste Manag. Assoc. 56 (6), 709–742. https://doi.org/10.1080/10473289.2006.10464485.

Prost, J., Wobrauschek, P., Streli, C., 2017. Quantitative total reflection X-ray fluorescence analysis of directly collected aerosol samples. X Ray Spectrom. 46 (5), 454–460. https://doi.org/10.1002/XRS.2752.

Ratoi, M., Niste, V.B., Alghawel, H., Suen, Y.F., Nelson, K., 2014. The impact of organic friction modifiers on engine oil tribofilms. RSC Adv. 4 (9), 4278–4285. https://doi.org/10.1039/c3ra46403b.

Ravel, B., Newville, M., 2005. ATHENA, artemis, hephaestus: data analysis for X-ray absorption spectroscopy using IFEFFIT. J. Synchrotron Radiat. 12 (4), 537–541. https://doi.org/10.1107/S0909049505012719.

Saarnio, K., Frey, A., Niemi, J.V., Timonen, H., Rönkkö, T., Karjalainen, P., Vestenius, M., Teinilä, K., Pirjola, L., Niemelä, V., Keskinen, J., Häyrinen, A., Hillamo, R., 2014. Chemical composition and size of particles in emissions of a coal-fired power plant with flue gas desulfurization. J. Aerosol Sci. 73, 14–26. https://doi.org/10.1016/j.jaerosci.2014.03.004.

Sakata, K., Sakaguchi, A., Tanimizu, M., Takaku, Y., Yokoyama, Y., Takahashi, Y., 2014. Identification of sources of lead in the atmosphere by chemical speciation using X-ray absorption near-edge structure (XANES) spectroscopy. J. Environ. Sci. (China) 26 (2), 343–352. https://doi.org/10.1016/S1001-0742(13)60430-1.

Solé, V.A., Papillon, E., Cotte, M., Walter, P., Susini, J., 2007. A multiplatform code for the analysis of energy-dispersive X-ray fluorescence spectra. Spectrochimica Acta - Part B Atomic Spectroscopy 62 (1), 63–68. https://doi.org/10.1016/j.sab.2006.12.002.

Tirez, K., Silversmit, G., Bleux, N., Adriaensens, E., Roekens, E., Servaes, K., Vanhoof, C., Vincze, L., Berghmans, P., 2011. Determination of hexavalent chromium in ambient air: a story of method induced Cr(III) oxidation. Atmos. Environ. 45 (30), 5332–5341. https://doi.org/10.1016/J.ATMOSENV.2011.06.043.

Vainikka, P., Hupa, M., 2012. Review on bromine in solid fuels - Part 2: anthropogenic occurrence. Fuel 94, 34–51. https://doi.org/10.1016/j.fuel.2011.11.021. Elsevier.

Valotto, G., Cattaruzza, E., Bardelli, F., 2017. Multi-edge X-ray absorption spectroscopy study of road dust samples from a traffic area of Venice using stoichiometric and environmental references. Spectrochim. Acta Mol. Biomol. Spectrosc. 173, 971–978. https://doi.org/10.1016/j.saa.2016.11.006.

Vekemans, B., Janssens, K., Vincze, L., Adams, F., Van Espen, P., 1994. Analysis of X-ray spectra by iterative least squares (AXIL): new developments. X Ray Spectrom. 23 (6), 278–285. https://doi.org/10.1002/xrs.1300230609.